Journal of Contaminant Hydrology 147 (2013) 34–44

Contents lists available at SciVerse ScienceDirect

Journal of Contaminant Hydrology

journal homepage: www.elsevier.com/locate/jconhyd

Effects of fluctuations in river water level on virus removal by bank filtration and aquifer passage — A scenario analysis

J. Derx [a,b,g,*], A.P. Blaschke [a,b,g], A.H. Farnleitner [c,b,g], L. Pang [d], G. Blöschl [a,b], J.F. Schijven [e,f]

[a] Institute of Hydraulic Engineering and Water Resources Management, E222/2, Karlsplatz 13 A-1040 Vienna, Austria
[b] Centre for Water Resource Systems (CWRS), Vienna University of Technology, Vienna, Austria
[c] Institute for Chemical Engineering, Research Area Applied Biochemistry and Gene Technology, Research Group Environmental Microbiology and Molecular Ecology, Vienna University of Technology, Vienna, Austria
[d] Institute of Environmental Science & Research Ltd., P.O. Box 29181, Christchurch, New Zealand
[e] Expert Centre for Methodology and Information Services, National Institute of Public Health and the Environment (RIVM), P.O. Box 1, 3720 BA Bilthoven, The Netherlands
[f] Department of Earth Sciences, Utrecht University, P.O. Box 80021, 3508 TA Utrecht, The Netherlands
[g] Interuniversity Cooperation Centre Water and Health, Vienna University of Technology, Austria [1]

ARTICLE INFO

Article history:
Received 22 July 2012
Received in revised form 28 December 2012
Accepted 3 January 2013
Available online 11 January 2013

Keywords:
Virus removal
River fluctuation
Riverbank filtration
Groundwater model
Dispersion

ABSTRACT

Riverbank filtration is an effective process for removing pathogenic viruses from river water. Despite indications that changing hydraulic conditions during floods can affect the efficacy of riverbank filtration to remove viruses, the impact on advection and dispersion of viruses in the riverbank is not well understood. We investigated the effects of fluctuations in river water level on virus transport during riverbank filtration, considering 3-D transient groundwater flow and virus transport. Using constant removal rates from published field experiments with bacteriophages, removal of viruses with distance from the riverbank was simulated for coarse gravel, fine gravel and fine sandy gravel.

Our simulations showed that, in comparison with steady flow conditions, fluctuations in river water level cause viruses to be transported further at higher concentrations into the riverbank. A 1–5 m increase in river water levels led to a 2- to 4-log ($\log_{10}$ reduction in concentration relative to the initial concentration in the river) increase in virus concentration and to up to 30 % shorter travel times. For particular cases during the receding flood, changing groundwater flow conditions caused that pristine groundwater was carried from further inland and that simulated virus concentrations were more diluted in groundwater. Our study suggests that the adverse effect of water level fluctuations on virus transport should be considered in the simulation of safe setback distances for drinking water supplies.

1. Introduction

Riverbank filtration is widely used as a treatment step for drinking water production, e.g., at the Ohio River (Weiss et al., 2005) and the Danube River (Homonnay, 2002). While water passes through the subsurface and travels to pumping wells, viruses undergo filtration and inactivation processes, which are determined by both the properties of aquifer media and the viruses (Schijven and Hassanizadeh, 2000). Virus concentrations in aquifer media were found to be strongly influenced by the aquifer heterogeneity (Maxwell et al., 2007), hydraulic conductivity, porosity and virus attachment (Barth and Hill, 2005). Virus removal processes may also be affected by pH, ionic strength (Sadeghi et al., 2011; Torkzaban et al., 2010), the redox conditions in groundwater (Schijven et al., 2000) and pore water velocity (Pang, 2009). In near-river aquifers, pore water velocity can vary significantly with a change in river water level, e.g., due to snow melting in spring and floods after heavy rainfalls (Shankar et al., 2009). Derx et al. (2010) demonstrated that

* Corresponding author at: Institute of Hydraulic Engineering and Water Resources Management, E222/2, Karlsplatz 13 A-1040 Vienna, Austria. Tel.: +43 158801 22223; fax: +43 158801 22399.
E-mail address: derx@waterresources.at (J. Derx).
[1] www.waterandhealth.at.

0169-7722/$ – see front matter © 2013 Published by Elsevier B.V.
http://dx.doi.org/10.1016/j.jconhyd.2013.01.001

fluctuations in river water level can lead to a larger dispersion of solutes in groundwater along the Danube riverbank. They explained the larger dispersion by spatially and temporally variable pore water velocities in the responding groundwater. The effect of river water level fluctuation on virus transport is yet unknown. We suspect that transient conditions of groundwater flow at riverbank filtration sites may affect the transport of viruses from the river water towards a pumping well. We hypothesize that an increase in river water level would lead to a larger dispersion of virus particles and thus to further transport during riverbank infiltration, similarly as found by Derx et al. (2010) for solutes. In addition, drainage and imbibition due to variable water tables or variable water saturation may remobilize previously deposited virus particles (Torkzaban et al., 2006).

Virus transport in heterogeneous gravel aquifers is significantly different from uniform sand media (e.g., beach sand aquifers). Virus transport in alluvial gravel aquifers occurs predominantly along preferential flow paths (Pang et al., 2005) and is faster and less dispersed than conservative chemical tracers due to size exclusion (Flynn, 2003). Riverbank alluvial deposits are typically non-uniform in grain sizes with a very wide particle size distribution, containing clay, silt, sand and gravel. Pang et al. (2005) found that the collision efficiency based on a singular grain size (Yao et al., 1971) did not apply well for describing virus transport in gravel aquifers. They recommended that it is best to use a first order removal rate rather than collision efficiencies to describe virus transport in heterogeneous gravel aquifers. First order law is the concept of numerous conventional transport models, implying concentration declines with distance exponentially and the reduction rate is a constant. Fitting a large amount of published field data on microbial transport in groundwater with both a first order law and a power law, Pang (2009) found that 70% of the data were better described with the first order law but 30% of the data (specially those from fine sediments) were better described with a power law (implying reduced removal rate with transport distance). The first order law was found to be applicable for (bio)colloid transport in gravel aquifer media Pang (2009).

Previous field studies on virus transport in groundwater were conducted to most parts under more or less steady flow conditions (Bales et al., 1995; Blanford et al., 2005; DeBorde et al., 1998, 1999; Pieper et al., 1997; Schijven et al., 2000, 2005; Woessner et al., 2001, see also Pang, 2009). In contrast to this previous work, this paper aims to contribute in examining virus transport during flooding events and specifically the role of varying pore water velocities on virus removal during riverbank filtration and aquifer passage. The secondary objective was to investigate the time scale at which river fluctuation affected virus transport. To achieve these objectives, we simulated virus transport into gravel and sandy gravel aquifers limited by a large river with high variations in river flow discharge, while keeping the rates of virus attachment, detachment and inactivation constant. Effects of clogging of the riverbed and pumping were studied as well. Finally, we discussed the general implications of the assumed scenarios.

2. Methods

For simulating virus transport during riverbank filtration and aquifer passage, we adapted the model setup outlined in Derx et al. (in press). In the following we describe this model setup in detail.

2.1. The hypothetical river and aquifer system

We considered shallow unconfined sandy gravel and gravel fluvial aquifers. These aquifers were assumed to be fully connected to the river or overlaid by a clogging layer on top of the riverbank and bed. A large river was simulated exhibiting large fluctuations in water levels with a maximum increase by 5 m. The corresponding river flow discharges ranged between 100 and 5700 m^3/s. Such flooding events could occur at large rivers on average once a year (e.g., at the River Danube, (via donau, 1997). These conditions are typical to riverbank filtration sites underlaid by fluvial gravel aquifers (Hoehn, 2002; Homonnay, 2002; Schubert, 2006; Weiss et al., 2005). See Section 2.4 for the adopted range of aquifer properties).

2.2. Water flow model

Groundwater flow and virus transport were simulated with a 3-D groundwater model (SUTRA2.1, Voss and Provost, 2008), coupled with a 1-D surface water model (HEC-RAS, U.S. Army Corps of Engineers, 2008). The near-river groundwater flow direction responded to a flood wave in the direction parallel and perpendicular to the river axis and in the vertical direction, as shown by the groundwater flow direction after 20 d of simulation time (Fig. 1). The 3-D governing equation for the transient variably saturated water flow is given below.

$$\left(\Theta_w \rho s_{op} + \Theta \rho \frac{\partial \Theta_w}{\partial p}\right) \cdot \frac{\partial p}{\partial t} - \nabla \left[\frac{\rho K(\Theta_w)}{\mu}(\nabla p + \rho \cdot \mathbf{g})\right] + q_w = 0. \quad (1)$$

Notations are given in Table 1.

The aquifer comprised an area of 9 by 4 km, limited by a straight river stretch of 9 km length (Fig. 1, left). The river boundary was 150 m wide, between the river center line and a steep river embankment. The dimensions of the aquifers were chosen large enough to avoid errors induced from boundary effects. The horizontal discretization of the numerical elements varied between 1.5 m and 100 m. Along the riverbanks and in the center of the assumed aquifers (gray shaded area in Fig. 1, left), smaller cell sizes were used to minimize the effect of numerical dispersion on transport simulations. The aquifer beneath the riverbed was 10 m deep and was discretized into 20 layers at an interval from 5 to 35 cm in the upper layers and 1.2–1.5 m in the lower layers (Fig. 1, right). Hydraulic conductivity (which represents conductance of the riverbed) was set homogeneously isotropic or vertically anisotropic (Section 2.4). To consider clogging processes, the uppermost 3 elements of the riverbed and riverbank were assigned to a fixed vertical cell size of 10 cm and a very low hydraulic conductivity of 10^{-5} to 10^{-6} m/s (Section 2.4). The model consisted of approximately 850,000 elements in total.

2.3. Boundary and initial conditions

In our simulations, a hydraulic gradient of 3 m/km was used to allow infiltration of river water to groundwater. A production well was placed at a distance of 100 m from the river (Fig. 1). The well consisted of horizontal collector pipes

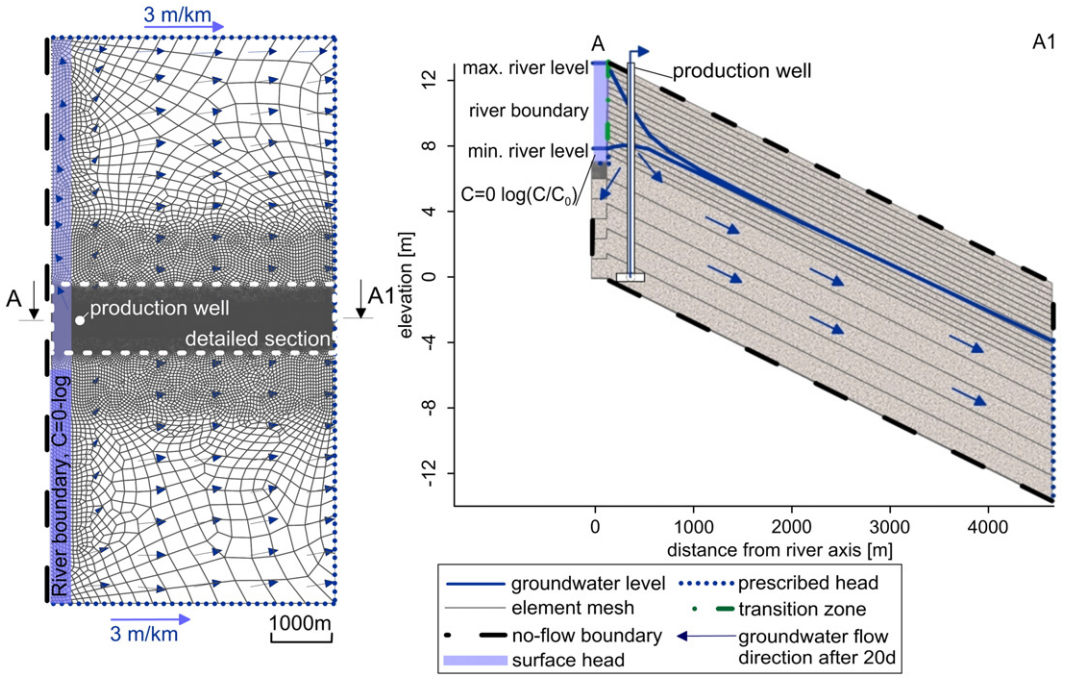

Fig. 1. Hypothetical aquifer scenario with boundary conditions (see legend) and simulated groundwater flow directions after 20 d (blue arrows). Map view shows the numerical mesh and detailed section (left); cross section A–A1 shows the maximum and minimum river levels together with simulated groundwater levels; The element sizes in vertical direction are indicated with fine solid lines (right).

Table 1
Notation.

C	Concentration of free viruses in groundwater (pfu/l) (pfu/l)
C_0	Concentration of free viruses in the river (pfu/l)
D	3-D dispersion matrix (m^2/s)
d_{req}	required distance to achieve a certain virus log reduction (m)
$\mathbf{g}$	Gravity vector [0,0,−9.81] (ms^{-2})
h	Aquifer depth (m)
Δd	Maximum element size (m)
Δh	Total difference in river level (m)
i	Hydraulic groundwater gradient (m/km)
K	3-D aquifer permeability matrix (m^2)
K_f	Hydraulic conductivity (m/s)
$K^*_{f,v/h}$	Anisotropy ratio of hydraulic conductivity (−)
n_{vg}	van Genuchten (1980) model parameter (−)
p	Hydraulic water pressure (kN/m^2)
p_e	*Peclet* number
pfu/l	Plaque forming units per liter
q_w	Fluid mass sink (mass fluid per time and volume aquifer, kg/m^3 s)
r^2_{lin}	Linear correlation coefficient (-)
ss	Scaled sensitivity (-)
s_{op}	Specific pressure storativity $(kg/ms^2)^{-1}$
t	Simulation time (d)
$\mathbf{v}$	Pore water velocity (m/d)
α_l	Longitudinal dispersivity (m)
α_t	Transversal dispersivity (m)
$\alpha^*_{v/h}$	Anisotropy ratio of dispersivity (−)
α_{vg}	van Genuchten (1980) model parameter (kPa^{-1})
λ	Virus temporal removal rate (d^{-1})
λ_s	Virus log removal rate ($\log_{10}$/m)
μ	Fluid viscosity (1.307×10^{-3} kg/ms at 10 °C)
∇	Differential operator (−)
ρ	Fluid density (999.7 kg/m^3 at 10 °C)
θ	Effective porosity (−)
θ_r	Residual water saturation (−)
θ_w	Water saturation (−)

extending radially at the bottom of the aquifer. This type of production well is commonly used in riverbanks for drinking water supplies because of its high yield capacities, for example at the Rhine or the Illinois River (Ray et al., 2002; Shankar et al., 2009). A constant pumping rate either of 0 or 100 L/s was assumed.

We assumed initial surface water depths of 0.5 m, 3 m and 5.5 m respectively. To generate the initial pressure heads, simulations were performed over a time long enough (1.5 years) holding all boundary conditions constant, so that the initial conditions had no influence on the groundwater flow results. The head boundary conditions along the river were based on the water levels predicted from the 1-D surface water model (blue shading in Fig. 1, left). Flood waves at the river boundary were simulated as continuous cosine functions with 1 m, 3 m and 5 m increases in river water levels and periods of 40 d (varied from 2 to 16 d for the sensitivity analysis). The dynamics of river flow and its effect on groundwater flow were fully accounted for. At all vertical boundaries, except the river boundary, the same constant head boundary conditions were applied as for the initial condition. The vertical boundary along the river axis was defined to be no-flow because parallel flow was assumed along this line. Likewise, the top layer in the land zone was set to no-flow, assuming no groundwater recharge from precipitation. Even though the slope of the top ground surface is usually directed towards the river, we chose the land slope parallel to the initial water pressure gradients assumed in the simulations, so that the groundwater level remained just below the land surface during the flooding events. This was done in order to avoid dispensable parts of the model. The

bottom boundary of the domain was defined to represent the aquitard.

The transition zone along the top surface of the riverbank between the highest and the lowest water mark alternated between submerged and dry (green dash–dotted line in Fig. 1, right). The boundary conditions in this zone were set according to the model result of the previous time step for a given node. If the hydraulic pressure of the previous time step was positive, the head boundary condition was set to the local surface water level. If the hydraulic pressure was negative, the boundary conditions were set to no-flow since the soil was unsaturated (Derx et al., 2010). All boundary conditions are shown in Fig. 1. The water flow model was tested for a field site at the Austrian Danube with transient flow conditions during several flooding events. The mean differences between measured and observed groundwater levels were always less than 7 cm (Derx et al., 2010). The transient groundwater flow situation during flooding events can be reproduced. The virus concentration C was simulated relative to the initial concentration in the river C_0. The aquifer was therefore assumed to be initially free of viruses. As concentration boundary condition at the river a constant virus concentration reduction of 0-log was assumed (Fig. 1, the river is shaded blue).

2.4. Aquifer properties/characteristics

Alluvial gravel aquifers near rivers often have hydraulic conductivity 10^{-3}–10^{-2} m/s (e.g., the River Rhine, Schubert, 2006 and Shankar et al., 2009). This range was used in the scenario simulations, including a clogging layer at the top 30 cm of the riverbank. In the sensitivity analysis a range in aquifer hydraulic conductivity from 10^{-4} to 10^{-2} m/s was considered. As clogging layers are typically rich of organic sediments, substantially higher virus removal rate coefficients were previously observed than in the surrounding aquifer sediments (Schijven and Hassanizadeh, 2000). In order to account for a substantial part of the virus log removal, we therefore assigned an extremely low hydraulic conductivity value of 10^{-7} m/s to this clogging layer. In addition, scenarios with a clogging layer at the uppermost 30 cm of the riverbed were also assumed with hydraulic conductivity of 10^{-6} m/s (referred to as *internal clogging* by Blaschke et al., 2003).

Similar characteristics of clogging layers have been observed e.g., at the Elbe River (Fischer et al., 2005) or at a bank filtration site near the Lake Tegel (Grünheid et al., 2005). In most cases, clogging processes may consist of several clogging cycles of a few weeks each initiated by floods until a stable state is reached (Blaschke et al., 2003). If the suspended load in the river is low, clogging will establish slowly and during long time periods. For simplicity, the clogging layers were therefore assumed to remain constant over time in the simulations. Anisotropy ratios of hydraulic conductivity and dispersivity of 0.1 were assumed for the scenarios and from 0.01 to 1 for the sensitivity analysis (Chen, 2000; Gelhar et al., 1992). We assumed a constant effective porosity of 0.1 in the scenarios and a range from 0.1 to 0.2 for the sensitivity analysis because only a fraction of the total porosity is effective for groundwater flow and transport (de Marsily, 1986). Water saturation and hydraulic conductivity in the unsaturated zone were calculated by using the model of van Genuchten (1980). The parameters α_{vg}, n_{vg} and the residual water saturation Θ_r were set to 0.36 kPa^{-1}, 3.18 and 0.14, as obtained by the *Rosetta Lite* program (Schaap et al., 2001) for the sand textural class of the USDA triangle. We additionally considered values for gravel, of 1.53 kPa^{-1}, 2 and 0.18, respectively, as determined from lab experiments by the Institute for Land and Water Management Research in Austria (unpublished data).

2.5. Virus transport model

Virus transport was simulated based on the advection–dispersion equation coupled with a first order removal rate (λ) by using SUTRA2.1:

$$\frac{\partial \Theta \Theta_w \rho C}{\partial t} = -\nabla(\Theta\Theta_w \rho v C) + \nabla(\Theta\Theta_w \rho D \nabla C) - \lambda \Theta\Theta_w \rho C. \quad (2)$$

Notations are given in Table 1. The dispersion tensor D in Eq. (2) is a product of the pore water velocity ($\mathbf{v}$), the longitudinal (α_l) and transversal dispersivity (α_t, Voss and Provost, 2008, Eq. 2.39d–2.40b). As a performance target, an 8-log reduction in virus concentration was selected, reducing enteric viruses from 100 pfu/l in wastewater to 10^{-6} pfu/l in groundwater (notations are given in Table 1). This level of reduction will approximately meet a health risk of 10^{-4} infections per person per year (Schijven et al., 2005). A 4-log reduction in virus concentration was also considered as a pretreatment step for drinking water production (USEPA, 2004).

Field experiments conducted in gravel and sandy gravel aquifers showed that virus surrogates were less dispersed than solute tracers because viruses travel through a narrower pore-network, e.g., by up to a factor of 3.5 (Pang et al., 2005). Thus the dispersivity values used in the simulations in this study were kept small to less than 5 m. Field experiments are preferably conducted in controlled steady flow conditions. Thus the dispersivity values used in the simulations in this study were kept small to less than 5 m to comply with what was observed in the field. Despite that the dispersivity remained constant during the simulations, the virus dispersion coefficients could vary due to variations in simulated pore water velocities. The transport behavior of virus surrogates during flooding may therefore be affected by additional dispersion in the near-river groundwater. The transversal dispersivity (α_t) was set to 0.2 α_l. In order to minimize numerical dispersion and ensure numerical stability, the following criterion was fulfilled: $p_e = v\Delta\, d/D \leq 2$ (Kinzelbach, 1987), notations are given in Table 1. This criterion was valid for small ratios of $\alpha_l/\alpha_t (<10)$ and for the three-dimensional case. As dispersivity values in gravel at the field scale are quite uncertain, a range of $\alpha_l = 5-50$ m was additionally considered (Section 2.6). Note that the dispersivity remained constant during the simulations, but the dispersion coefficient could vary due to variations in river water levels and pore water velocities.

Virus removal rates (λ) were adapted from the removal rates of MS2 and PRD1 bacteriophages that Pang (2009) derived from 11 published field experiments conducted in fine gravel aquifers (Table 2). We selected MS2 andPRD1 as model viruses, as they are about equally conservative for attachment (Schijven and Hassanizadeh, 2000). In order to use these rates in model simulations, the spatial removal rates (λ_s) reported in Pang (2009) were converted to temporal

removal rates (λ) by $\lambda = 2.3v\lambda_s$ (Pang, 2009, Eq. (3)), where **v** were the minimum pore water velocities reported in the published field experiments. A factor of 2.3 was added for the conversion of λ from log/d into ln/d. This gave the virus removal rates, ranging from 0.07 d^{-1} to 10.15 d^{-1}, with a median of 0.9 d^{-1} (Table 2). The removal rates were assumed to be constant. The respective minimum pore water velocities observed during these experiments ranged from 0.2 m/d to 147 m/d (Table 2). The respective values demonstrate that there is a clear relationship of virus removal rates to pore water velocities which is in accordance with the colloid filtration theory (Yao et al., 1971).

Note that the spatial removal rates reported in Pang (2009) comprised not only attachment and inactivation but also some effect of dilution. This is because a removal rate was derived from the slope of $\log_{10}(C_{max}/C_0)$ versus distance plot (excluding the injection well). When bromide data are available in the published experiments, the slope of $\log_{10}(C_{max}/C_0)$ versus the distance plot for bromide reflects the effect of dilution. Thus the net removal rate induced from the attachment and inactivation of the virus was then revised by subtracting the bromide slope from that of the virus (Table 2). No inactivation was additionally considered in the simulations as it had been already lumped into the total removal rate. The contribution of inactivation to total removal is expected to be insignificant due to the relatively short travel times in the simulations. Schijven and Hassanizadeh (2000) showed that virus inactivation could be very low $\leq 0.1\,d^{-1}$ even at summer water temperatures for persistent viruses.

The transport model was tested and verified for several 2-D/3-D solute transport problems by Voss and Provost (2008). In order to test the simulations with the first order concentration reduction, a simple box model was set up. Initial solute concentrations at one uniform value were assigned throughout the box and a first order decay rate was specified. The concentration reduced exponentially with time (results not shown).

2.6. Scenarios and sensitivity analysis

Table 3 lists all scenarios that we applied (12 cases). In the scenarios, river levels were assumed to be constant, fluctuating with 1 m head difference for 20 times, or two large flow events were simulated, with 3 m and 5 m of maximum head increase in the river. The flood waves were simulated to last for 20 days followed by 40 days of steady low flow conditions.

Table 3
Hypothetical aquifer scenarios assumed and corresponding figures for simulation results. Each scenario was simulated in coarse gravel, fine gravel and fine, sandy gravel, with an increase of river water level by 0, 1, 3 and 5 m.

Pumping rate	Clogging	α_l	Figures
0	No	≤5	4 (top), 2
100	No	≤5	4 (middle)
0	Yes	≤5	4 (bottom)
0	Yes	20	5

The hydraulic conductivity (K_f) and virus removal rate (λ) were assigned to coarse gravel ($K_f = 10^{-2}$ m/s, $\lambda = 0.07\ d^{-1}$), fine gravel ($K_f = 5 \cdot 10^{-3}$ m/s, $\lambda = 0.90\ d^{-1}$) and fine sandy gravel ($K_f = 10^{-3}$ m/s, $\lambda = 10.15\ d^{-1}$). The largest virus removal rate was assigned to the finest material because of a higher affinity to attach to sediments. Also, higher dispersivity values, clogging of the riverbank or riverbed and a pumping rate of 100 L/s were included in the scenarios (Table 3).

In the sensitivity analysis, one parameter at a time was changed within the range given in Sections 2.4, 2.5 and Table 2, while holding all other parameters constant at median values. In order to investigate the effect of the flood duration on virus removal during riverbank filtration, flood waves were additionally simulated to last for 1, 2, 3, 4 and 8 days. Simulations were carried out just long enough to simulate 2 cycles of river water level fluctuation (16 d). The estimated distances for virus concentration reduction gave the opportunity to compare the effects of the parameters relatively to each other. The sensitivity analysis used followed the general procedures described in Hill (1998). One-percent scaled sensitivities (1%ss) were calculated which reflect the amount that simulated required distances for 8-log virus concentration reduction would change if a parameter value increased by 1% (see Hill, 1998, Eq. 11).

3. Results

As the purpose of this study was to investigate the effects of fluctuations in river water level on virus transport in

Table 2
Calculation of virus removal rates from field data encompassing the full range observed in sandy gravel and gravel media with MS2 and PRD1 bacteriophage tracers (Pang, 2009); Bold λ values relate to values after correction for dilution and indicate the maximum or minimum values considered in the simulations; For the sensitivity analysis, the considered ranges were extended by a value for *poliovirus* (Section 2.6).

Reference	Source	Aquifer	Phage	λ_s ($\log_{10}$/m)	v_{min} (m/d)	λ (d^{-1})	$r^2_{lin.}$ (−)	No. (−)	Dilution corr.
Bales et al. (1995)	Sewage	Sand, fine gravel	PRD-1	0.18	0.2	**0.07**	0.83	6	Yes
Blanford et al. (2005)	Sewage	Sand, fine gravel	PRD-1	0.89	0.5	1.09	lin.	31	No
Blanford et al. (2005)	Sewage	Sand, fine gravel	PRD-1	0.11	0.5	0.13	lin.	21	No
Blanford et al. (2005)	Tracer	Sand, fine gravel	PRD-1	0.12	0.5	0.14	lin.	32	No
DeBorde et al. (1998)	Septic tanks	Sand, gravel	MS2	0.39	1.0	0.90	0.84	3	No
DeBorde et al. (1999)	Tracer	Sandy gravel	MS2	0.10	23.0	5.26	0.99	4	No
DeBorde et al. (1999)	Tracer	Sandy gravel	PRD-1	0.09	26.0	5.66	0.98	4	No
Pieper et al. (1997)	Tracer	Sand, fine gravel	PRD-1	0.22	0.8	0.40	0.77	4	No
Pieper et al. (1997)	Sewage	Sand, fine gravel	PRD-1	0.21	0.4	0.20	0.43	4	No
Woessner et al. (2001)	Tracer	Sand, gravel	PRD-1	0.01	115	3.19		1	No
Woessner et al. (2001)	Tracer	Sand, gravel	MS2	0.04	147	**10.15**		1	Yes
Woessner et al. (2001)	Clean	Sand and gravel	Poliovirus	0.14	172	53.80		1	No

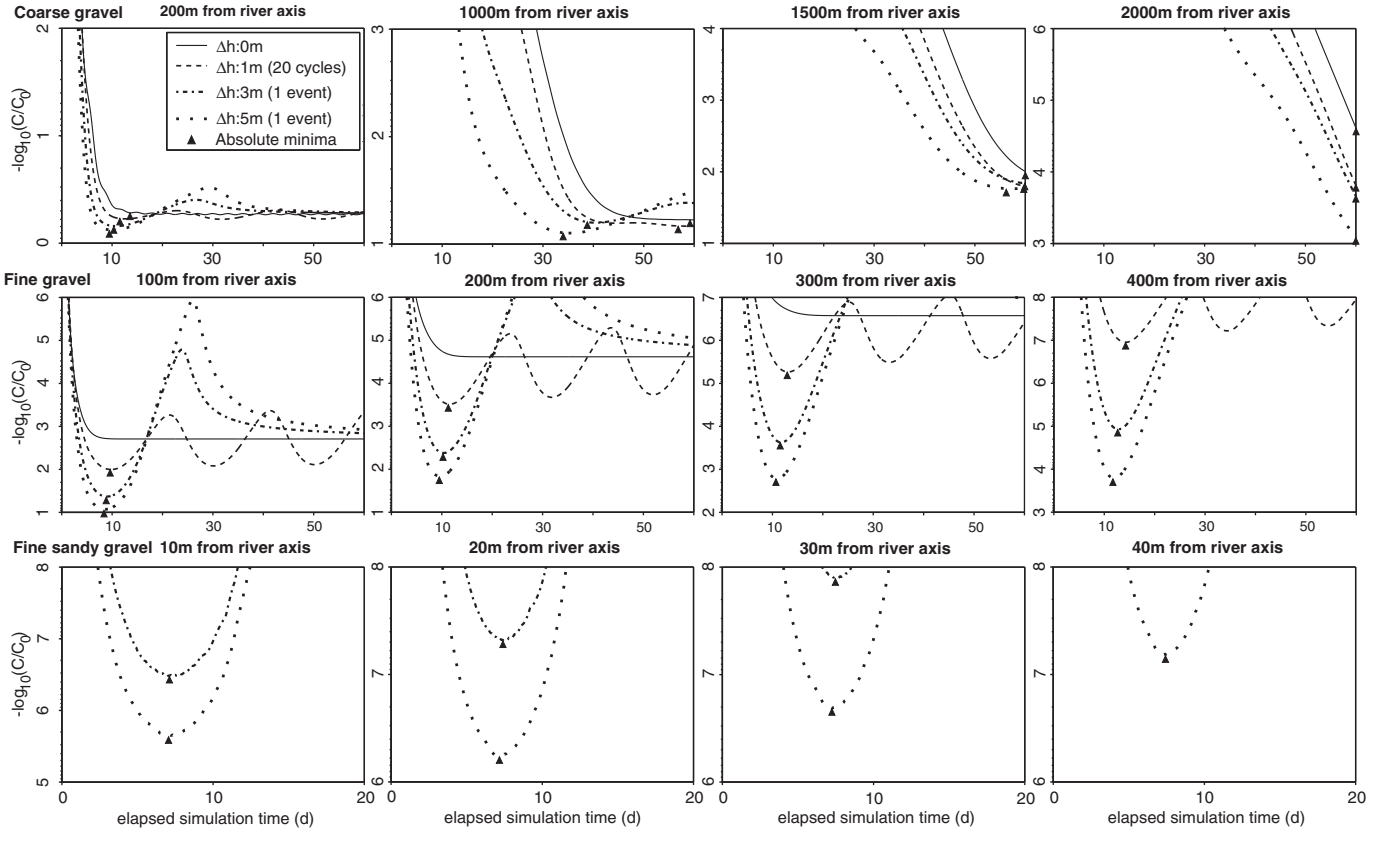

Fig. 2. Simulated virus concentration reductions at various distances from the river, estimated from simulations in coarse gravel, fine gravel and fine sandy gravel material, simulated with head changes in the river (Δh) of 0 m,1 m, 3 m and 5 m; pumping rate: 0 L/s.

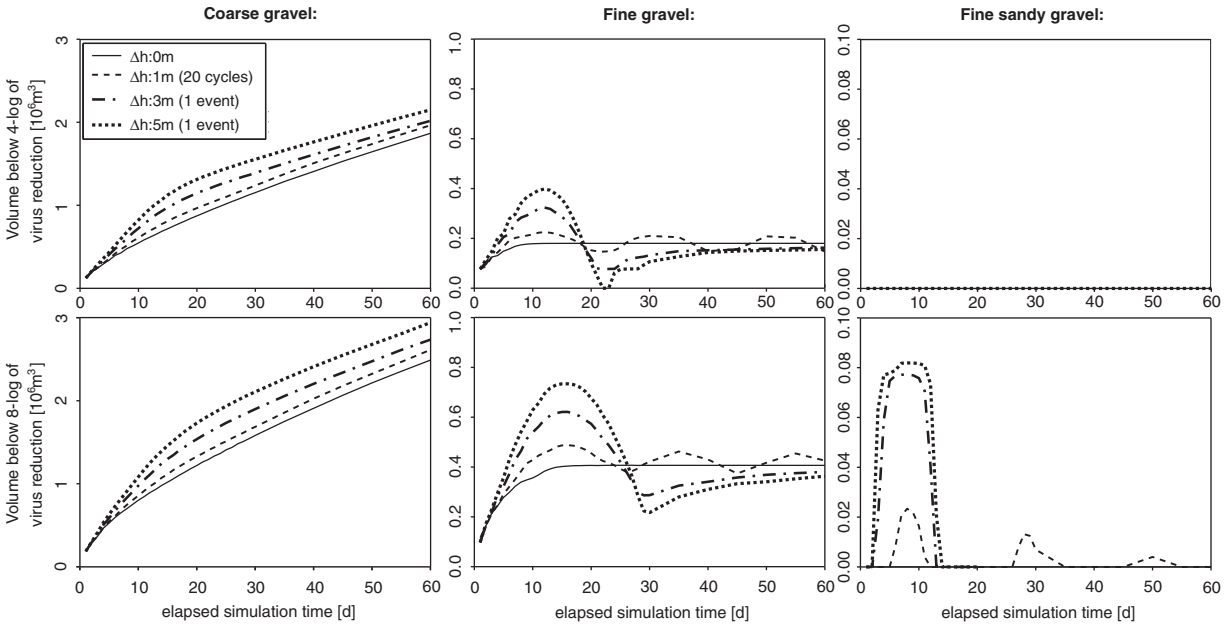

Fig. 3. Volumes below 4-log (top) and 8-log (bottom) of virus concentration reductions, estimated from the simulations in Fig. 2; the volumes were calculated for the detailed section shown in Fig. 1.

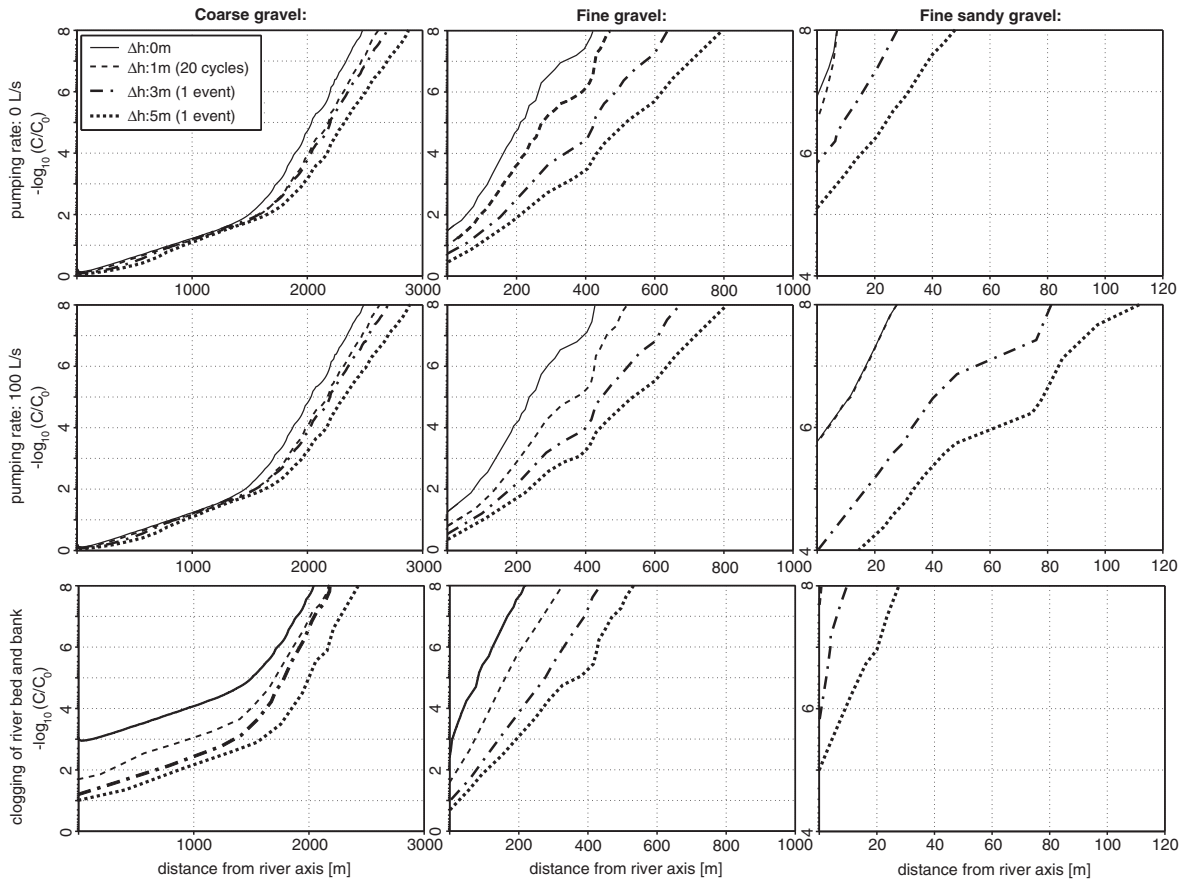

Fig. 4. Minimum virus concentration reductions after 60 d versus distance from the river axis (as indicated in Fig. 2), estimated from the simulations in Figs. 2 and 3 (top). A pumping rate of 100 L/s was assumed (middle) and a 30 cm clogging layer on top of the river bank ($K_f = 10^{-7}$ m/s) and the river bed (K_f = m/s) (bottom).

groundwater, we simulated groundwater flow with a hydraulic gradient directed from the river into groundwater and virus concentrations (C) relative to the river (C_0). Fig. 2 shows the log virus concentration reduction over time. These results can also be read as a virus concentration relative to C_0, where high reductions are equivalent to low concentrations. In the scenarios with flood waves, the hydraulic gradients near the river increased during rising river water levels (days 0–10), leading to a higher fraction of infiltrated river water in the aquifer. An increase in river water level by 5 m caused the simulated virus peak concentrations to be reduced less effectively than during steady flow conditions, by up to 4-log at 400 m from the river axis in fine gravel (Fig. 2). The larger the flood wave, the smaller the virus removal efficacy. The simulations further showed that flood waves can lead to an earlier arrival of virus peak concentrations in groundwater. For example, simulated virus peak concentrations in coarse gravel at 1000 m from the river arrived by 19 d (30%) earlier than during steady flow conditions.

In order to investigate the effects of river water level fluctuations on virus concentration reductions in a more quantitative way, the volumes below certain thresholds of concentration reduction for every day of simulation time were calculated (4-log and 8-log). The results were compared between transport simulations, where the river water levels were held constant and where river water levels increased by 1, 3 and 5 m. (Fig. 3). The calculated maximum volumes for a threshold of 8-log concentration reduction were 2.4 (coarse gravel), 0.4 (fine gravel) and $0.01 \cdot 10^6$ m^3 (fine sandy gravel) in the case of constant river water levels, as compared to 2.9, 0.7 and $0.08 \cdot 10^6$ m^3, respectively, for river water level increases by 5 m (Fig. 3, bottom). This means that the river water fluctuations increase the size of the virus concentration volume by a factor of 1.2 to 8.

After a certain simulation time (e.g., 40 d in coarse gravel at 200 m from the riverbank), the simulated virus concentrations at a given distance reached a semi-steady state, while fluctuating between fixed water levels (Figs. 2 and 3). For scenarios where river water levels fluctuated only once during a larger flow event (≥3 m), virus concentrations reached a steady-state more quickly.

For coarse gravel the simulated virus concentrations were less influenced by river water level fluctuation as compared to fine gravel (Figs. 2 and 3). As simulated virus concentrations reached further into groundwater, it took longer in reaching a steady state. This can be seen in Fig. 4 left, where the minimum simulated virus concentration reductions after 60 d sharply increased at 1500 m from the riverbank. Obviously, the simulated virus concentrations had already approached the final, steady-state closer to the riverbank (0–1500 m), but had not yet approached a steady-state further away from the riverbank.

During the receding flood, there was a natural groundwater gradient towards the riverbank, as shown by the simulated groundwater flow directions after 20 d (Fig. 1). Such conditions often occur if the river water level decreases faster than the groundwater levels nearby the river, leading to a dilution effect of virus contamination (e.g., Derx et al., in press; Shankar et al., 2009). In our simulations, the simulated virus concentrations were consequently more affected by dilution in fine gravel (Fig. 2).

Figs. 4–5 show the minimum virus concentration reductions in the aquifer with distance from the river axis. For all soil materials, the simulations showed that the reductions in virus concentration after increases in river water levels by 1–5 m are lower than during the steady flow conditions (Fig. 4).

During the steady flow conditions, the required distances from the river to achieve a respective 4(8)-log virus reduction performance target were 1900(2400) m in coarse gravel, 170(410) m in fine gravel and 0(8) m in fine sandy gravel (Fig. 4). The simulations indicated that an increase in river water level amplitude by 1, 3 and 5 m can require by 5, 10 and 15% greater distances from the river to achieve a 4- or 8-log virus reduction performance target in coarse gravel, respectively. For fine gravel the simulations indicated by 10, 50 and 90% greater distances and for fine sandy gravel, by 0, 300 and 500% greater distances than during steady flow conditions (Fig. 4). When varying the initial river water depth from 0.5 to 5.5 m during steady flow conditions, the simulated virus concentrations were identical (results not shown).

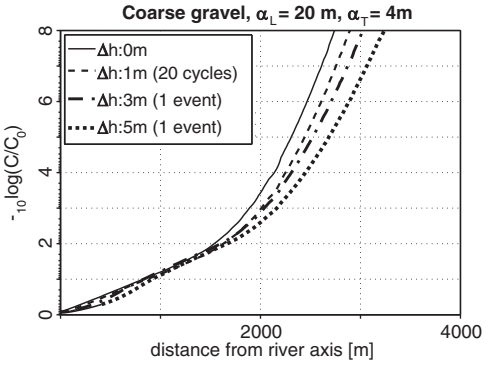

Fig. 5. Same as Fig. 4, but for a heterogeneous aquifer ($\alpha_L = 20$ m, $\alpha_T = 4$ m).

Table 4
Simulation results of the sensitivity analysis; Required distances (d_{req}) from the riverbank to achieve an exemplary 8-log virus reduction performance target after 16 d of simulation time for different values of the most influential parameters (center); One-percent scaled sensitivites (1% ss, Section 2.6, right). Two values refer to results for steady flow conditions ($\Delta h = 0$ m) and to results with fluctuating river water levels ($\Delta h = 3$ m).

Parameter values	d_{req}	1% ss
	[m]	[−]
$\Delta h_{=}$0 m	215	0.0
$\Delta h_{=}$1 m	215	0.1
$\Delta h_{=}$3 m	271	0.8
$\Delta h_{=}$5 m	322	1.3
$\alpha_l = \leq$5 m	215/271	0.4/0.2
$\alpha_l = 10$ m	256/293	0.6/0.4
$\alpha_l = 50$ m	392/454	1.6/1.7
$\alpha_l = 100$ m	531/600	2.8/2.9
$K_f = 10^{-4}$ m/s	35/85	0.2/0.2
$K_f = 10^{-3}$ m/s	215/271	1.5/1.5
$K_f = 10^{-2}$ m/s	1053/1074	9.3/8.9
$\lambda = 0$ d^{-1}	215/271	0.0/0.0
$\lambda = 0.08$ d^{-1}	215/263	0.0/−0.1
$\lambda = 1.3$ d^{-1}	85/121	−0.7/−0.8
$\lambda = 53.8$ d^{-1}	2/12	−0.9/-1.1
$\Theta = 0.1$	215/271	−1.0/−1.1
$\Theta = 0.15$	167/215	−1.1/−1.2
$\Theta = 0.2$	140/192	−1.1/−0.9

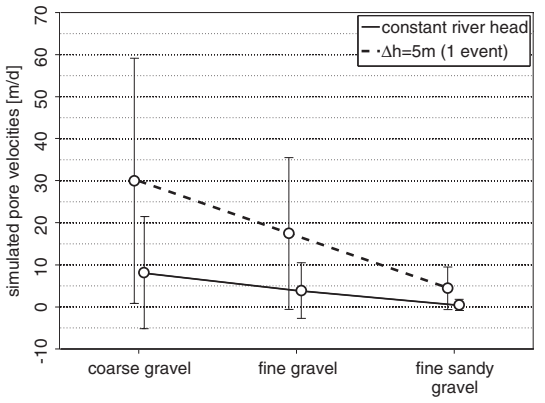

Fig. 6. Simulated average pore water velocities after an increase in river water level by 5 m (dashed line) and during steady flow conditions (solid line, estimated from simulations in Figs. 2–4 top); standard deviations are indicated.

A pumping rate of 100 L/s from a well caused hydraulic gradients to increase in the affected area, thus obviously enhancing virus infiltration from the river into the bank. The scenarios with pumping during steady flow conditions showed that virus can travel consequently further into groundwater relative to conditions without pumping and that virus concentrations are reduced less effectively, by up to 0.3-log in fine gravel and by up to 2-log in fine sandy gravel (Fig. 4).

The effects of river water level fluctuation on simulated virus concentrations were the same as without pumping. Due to the vicinity of the assumed well to the river and as the simulated travel distance was much further in coarse gravel, pumping had no effect for the scenarios in coarse gravel (Fig. 4).

The presence of a 30-cm clogging layer on top of the riverbank had a negligible effect on the simulated virus concentrations (not shown). Obviously, most of the river water infiltrates through the 150 m wide river bed rather than through the 10 m wide riverbank. When both the riverbed and the riverbank were assumed to be overlaid by a clogging layer, virus concentrations were reduced by 1 to 3-log within this first layer of sediments. For the remaining part of virus log reductions, the simulations indicate that an increase in river water level fluctuation can cause virus concentrations to be reduced less effectively, by up to 5-log at 200 m from the river axis in fine gravel (Fig. 4, bottom). For more heterogeneous aquifer scenarios (larger dispersivity values), the simulations showed the same effect of river water level fluctuation on required distances from the river as for scenarios with small dispersivities (Fig. 4). Viruses were generally transported 15% further into the riverbank (Fig. 5).

The results of the sensitivity analysis indicated that the most influential parameters on the required distance from the river for virus removal are aquifer hydraulic conductivity, followed by aquifer dispersivity, amplitudes of river water level fluctuation, virus removal rate and effective porosity (see 1-% scaled sensitivities in Table 4). The duration of the flooding events hardly affected the simulated required distance for virus removal (results not shown). Variations in anisotropy ratios for $K^*_{f,v/h}$ or $\alpha^*_{v/h}$ did not affect the simulated virus concentrations. Also variations in water saturation and in the parameters for the unsaturated zone had small effects on simulated virus concentrations.

The absolute pore water velocities during the simulations ranged between 0 m/d and 60 m/d (Fig. 6). This is within the range of pore water velocities observed during the field experiments that we used for deriving virus removal rate coefficients for the simulations (Table 2). The effects of pore velocity on virus removal are thus included in the simulations.

4. Discussion

4.1. Effects on virus removal and transport time scale

The primary objective of this paper was to investigate the effect of fluctuations in river water levels on virus transport and removal during riverbank filtration and aquifer passage. The largest effects of river water level fluctuation were generally shown for the finest gravel. Both higher advection during rising river levels and more dispersion were responsible for these effects. Due to the accumulative dispersion effect with travel distance, the flood waves led to a decreasing virus removal efficacy with increasing distance from the river. More dispersion resulted from the river water level fluctuations, which caused variations in pore water velocities (Fig. 6), similarly as found by Derx et al. (2010) for a field site at the River Danube for conservative tracers. The river water levels increased by 1 m in the study site of Derx et al. (2010), leading to 3 times greater volumes of tracer plumes infiltrating from the river into groundwater. At the Danube field site, the presence of bed form heterogeneities may have additionally facilitated solute transport into groundwater (Storey et al., 2003). As virus transport in gravelly types of aquifers occurs predominantly along preferential flow paths, this may additionally affect virus dispersion in groundwater during floods. We used small dispersivity values to account for a smaller dispersivity which was observed for virus surrogates as compared to conservative tracers (Pang et al., 2005). An alternative approach would be to use non-equilibrium transport models and kinetic transfer rates between mobile-and immobile zones, as e.g., were used for simulating *Salmonella* bacteriophage experiments by Pang et al. (2008). Lu et al. (2009) investigated the effect of the kinetic transfer rate on solute transport by using a similar approach as Pang et al.'s (2008), but for coastal aquifers during tidal fluctuation. Simulations by Lu et al. (2009) showed that kinetic mass transfer may significantly widen the mixing zone. Specifically, they showed that the maximum width of the mixing zone may occur if the mean retention time scale of solutes in the immobile zone is comparable to the period of water level fluctuations. In cases when virus desorption is more relevant and if virus transport occurs predominantly along preferential flow paths, virus concentrations may therefore be even more dispersed in the near-river groundwater than shown in our simulations. This would require further investigation in the future.

A secondary objective was to investigate the time scale at which river water level fluctuation affected virus transport. The simulations indicated that the amplitudes of river water levels are the most important for virus transport and that the duration and frequency of the river floods are of minor importance. Similarly, multiple tidal cycles caused enhanced mixing at a seawater site (Robinson et al., 2006), while one flooding event sufficed to cause enhanced mixing at a Danube site (Derx et al., 2010). Two or more consecutive

flooding events may therefore have similar effects on virus transport than one single event. Frequent flooding events occur for example during the monsoon season at the Brahmaputra River (Sarma, 2005).

Our simulations further indicated that temporary changes in groundwater flow direction (i.e., from infiltration to groundwater exfiltration) can compensate the adverse effects of river water level fluctuation on virus removal during riverbank filtration. Such effects of dilution occur under conditions that pristine groundwater is carried from further inland regions.

5. General implications of the assumed scenarios

In this paper, the investigated transient processes are restricted to water level fluctuations and hydraulic flow dynamics, so virus removal rates were kept constant. The aim was to investigate this transient process of water level fluctuation on the dispersion of the transported virus. River water level and groundwater level fluctuations, however, may also lead to remobilization of deposited colloids, including virus particles (Torkzaban et al., 2006). This requires virus removal rate to be a function of water saturation, which is another transient process (Sen, 2011). Unsaturated flow and transport become more important in the case of major floodings and inundation of overland areas or during strong precipitation events. In this paper, however, we focused on more frequent flooding events at a regulated river and have not considered overland flows. Virus removal rates may also vary in time and space due to changes in water chemistry and pore water velocities. Geochemical conditions can range from favorable to unfavorable for virus attachment to soil particles and also geophysical conditions can range, so it is very important to know the location-specific conditions. The aim of our simulations, however, was to investigate the process and effect of hydraulic flow dynamics.

For our scenarios virus concentrations at the river boundary were also assumed constant in time. Virus concentrations in the river, however, may be elevated after flooding events, as observed e.g., in the River Rhine by Schijven and de Roda Husman (2005). In this case more virus particles could enter the aquifer and a flood wave would facilitate virus transport during bank filtration even more. On the other hand, the dilution during high river water levels can be enormous in large rivers and may outweigh the greater total number of viruses in the river.

Our scenarios indicated that the simulated virus transport into groundwater is the same for constant high or low river water levels. This is because identical hydraulic pressure gradients were assumed during steady flow conditions, which are an important process controlling the river–aquifer interaction (Storey et al., 2003). While we assumed that the flow direction is generally from the river into groundwater for our scenarios, groundwater is often exfiltrating during low flow conditions or when pumps are turned off (Sheets et al., 2002). During flood events, however, virus transport is likely to be most affected by the change in river water level during the flood, rather than the groundwater situation before the flood. Our simulations therefore also apply for situations where groundwater is exfiltrating into the river during low flow conditions.

6. Conclusion

Our simulations indicate that flooding events cause viruses to be transported further and at higher concentrations into groundwater during riverbank filtration and aquifer passage. A 1–5 m increase in river water levels led to an increase in virus concentration volumes in groundwater by a factor of 1.2 to 8 (or to a 2- to 4-log higher virus concentration) and to up to 30% shorter travel times. A temporary change of groundwater flow direction during the receding flood can cause pristine groundwater to be carried from further inland and that virus concentrations are more diluted in groundwater. The amplitudes of river water levels were the most important for the simulated virus transport, while the duration and frequency of the river floods were less relevant. In this paper we considered groundwater flow and transport in three dimensions, as we especially focused on the effects of dispersion which may be smaller when considering less dimensions. In order to estimate the required distance for a given situation, detailed specific data (pore water velocities, removal rate, virus concentrations in river water) are essential. In future field studies, these effects and also effects of variations in water chemistry on virus transport need to be further investigated. It will hence be important to monitor a change in chemical water composition, water saturation and flow velocities during floods, as they have important influence on virus removal.

Acknowledgments

This paper was supported by the Austrian Science Fund (FWF) as part of the DKplus (Vienna Doctoral Program on Water Resource Systems, W1219-N22) and the GWRS-Vienna in cooperation with Vienna Water as part of the "(New)Danube – Untere Lobau Network Project" (Gewässervernetzung (Neue) Donau – Untere Lobau (Nationalpark Donau-Auen) funded by the Government of Austria (Federal Ministry of Agriculture, Forestry, Environment & Water Management), the Government of Vienna, and the European Agricultural Fund for Rural Development (project LE 07-13). This publication was developed within the Interuniversity Cooperation Centre Water and Health (ICC Water & Health, www.waterandhealth.at).

References

Bales, R., Li, S., Maguire, K., Yahya, M., Gerba, C., Harvey, R., 1995. Virus and bacteria transport in a sandy aquifer, Cape Cod, MA. Ground Water 33, 653–661.

Barth, G., Hill, M., 2005. Parameter and observation importance in modelling virus transport in saturated porous media — investigations in a homogeneous system. Journal of Contaminant Hydrology 80, 107–129.

Blanford, W., Brusseau, M., Yeh, T., Gerba, C., Harvey, R., 2005. Influence of water chemistry and travel distance on bacteriophage PRD-1 transport in a sandy aquifer. Water Research 39, 2345–2357.

Blaschke, A., Steiner, K.H., Schmalfuss, R., Gutknecht, D., Sengschmitt, D., 2003. Clogging processes in hyporheic interstices of an impounded river, the Danube at Vienna, Austria. International Review of Hydrobiology 88, 397–413.

Chen, X., 2000. Measurement of streambed hydraulic conductivity and its anisotropy. Environmental Geology 39, 1317–1324.

de Marsily, G., 1986. Quantitative Hydrogeology. Academic Press, New York.

DeBorde, D., Woessner, W., Lauerman, B., Ball, P., 1998. Virus occurrence and transport in a school septic system and unconfined aquifer. Ground Water 36, 825–834.

DeBorde, D., Woessner, W., Kiley, Q., Ball, P., 1999. Rapid transport of viruses in a floodplain aquifer. Water Research 33, 2229–2238.

Derx, J., Blaschke, A.P., Blöschl, G., 2010. Three-dimensional flow patterns at the river–aquifer interface — a case study at the Danube. Advances in Water Resources 33, 1375–1387.

Derx, J., Farnleitner, A.H., Zessner, M., Pang, L., Schijven, J., Blaschke, A.P., in press. Evaluating the effect of temperature induced water viscosity and density fluctuations on virus and DOC removal during river bank filtration — a scenario analysis, River System.

Fischer, T., Day, K., Grischek, T., 2005. Sustainability of riverbank filtration in Dresden, Germany. 5th International Symposium on Management of Aquifer Recharge. ISMAR, UNESCO, Berlin, Germany, pp. 23–28.

Flynn, R., 2003. Virus transport and attenuation in perialpine gravel aquifers, Ph.D. thesis, University of Neuchâtel, Switzerland.

Gelhar, L., Welty, C., Rehfeldt, K., 1992. A critical review of data on field-scale dispersion in aquifers. Water Resources Research 28, 1955–1974.

Grünheid, S., Amy, G., Jekel, M., 2005. Removal of bulk dissolved organic carbon (DOC) and trace organic compounds by bank filtration and artificial recharge. Water Research 3219–3228.

Hill, M., 1998. Methods and guidelines for effective model calibration. Technical Report Water-Resources Investigations Report 98-4005. (Denver, Colorado).

Hoehn, E., 2002. Hydrogeological issues of riverbank filtration — a review. In: Ray, C. (Ed.), Riverbank Filtration: Understanding Contaminant Biogeochemistry and Pathogen Removal. NATO Scientific Affairs Division, pp. 17–41.

Homonnay, Z., 2002. Use of bank filtration in Hungary. In: Ray, C. (Ed.), Riverbank Filtration: Understanding Contaminant Biogeochemistry and Pathogen Removal. NATO Scientific Affairs Division.

Kinzelbach, W., 1987. Numerische Methoden zur Modellierung des Transports von Schadstoffen im Grundwasser. R. Oldenbourg Verlag, München Wien.

Lu, C., Kitanidis, P.K., Luo, J., 2009. Effects of kinetic mass transfer and transient flow conditions on widening mixing zones in coastal aquifers. Water Resources Research 45.

Maxwell, R., Welty, C., Harvey, R., 2007. Revisiting the Cape Cod bacteria injection experiment using a stochastic modeling approach. Environmental Science and Technology 41, 5548–5558.

Pang, L., 2009. Microbial removal rates in subsurface media estimated from published studies of field experiments and large intact soil cores. Journal of Environmental Quality 38, 1–12.

Pang, L., Close, M., Goltz, M., Noonan, M., Sinton, L., 2005. Filtration and transport of *Bacillus subtilis* spores and the F-RNA phage MS2 in a coarse alluvial gravel aquifer: implications in the estimation of setback distances. Journal of Contaminant Hydrology 77, 165–194.

Pang, L., McLeod, M., Aislabie, J., Šimůnek, J., Close, M., Hector, R., 2008. Modeling transport of microbes in ten undisturbed soils under effluent irrigation. Vadose Zone Journal 7, 97–111.

Pieper, A., Ryan, J., Harvey, R., Amy, G., Illangasekare, T., Metge, D., 1997. Transport and recovery of bacteriophage PRD1 in a sand and gravel aquifer: effect of sewage-derived organic matter. Environmental Science and Technology 31, 1163–1170.

Ray, C., Soong, T., Lian, Y., Roadcap, G., 2002. Effect of flood-induced chemical load on filtrate quality at bank filtration sites. Journal of Hydrology 266, 235–258.

Robinson, C., Gibbes, B., Li, L., 2006. Driving mechanisms for groundwater flow and salt transport in a subterranean estuary. Geophysical Research Letters 33, 1–4.

Sadeghi, G., Schijven, J., Behrends, T., Hassanizadeh, S., Gerritse, J., Kleingeld, P., 2011. Systematic study of effects of pH and ionic strength on attachment of phage PRD1. Critical Reviews in Environmental Science and Technology 49, 12–19.

Sarma, J., 2005. Fluvial process and morphology of the Brahmaputra River in Assam, India. Geomorphology 70.

Schaap, M.G., Leij, F.J., Van Genuchten, M.T., 2001. ROSETTA: a computer program for estimating soil hydraulic parameters with hierarchical pedotransfer functions. Journal of Hydrology 251, 163–176.

Schijven, J., de Roda Husman, A., 2005. Effect of climate changes on waterborne disease in The Netherlands. Water Science and Technology 51, 79–87.

Schijven, J.F., Hassanizadeh, S., 2000. Removal of viruses by soil passage: overview of modeling, processes and parameters. Critical Reviews in Environmental Science and Technology 30, 49–127.

Schijven, J., Medema, G., Vogelaar, A., Hassanizadeh, S., 2000. Removal of microorganisms by deep well injection. Journal of Contaminant Hydrology 44, 301–327.

Schijven, J., Rijs, G., de Roda Husman, A., 2005. Quantitative risk assessment of FMD virus transmission via water. Risk Analysis 25, 13–21.

Schubert, J., 2006. Significance of hydrologic aspects on RBF performance. In: Hubbs, S. (Ed.), Riverbank Filtration Hydrology, pp. 17–41.

Sen, T., 2011. Processes in pathogenic biocolloidal contaminants transport in saturated and unsaturated porous media: a review. Water, Air, and Soil Pollution 216, 239–256.

Shankar, V., Eckert, P., Ojha, C., König, C., 2009. Transient three-dimensional modeling of riverbank filtration at Grind well field, Germany. Hydrogeology Journal 17, 321–326.

Sheets, R., Darner, R., Whitteberry, B., 2002. Lag times of bank filtration at a well field, Cincinnati, Ohio, USA. Journal of Hydrology 266, 162–174.

Storey, R., Howard, K., Williams, D., 2003. Factors controlling riffle-scale hyporheic exchange flows and their seasonal changes in a gaining stream: a three-dimensional groundwater flow model. Water Resources Research 39 (2), 1034.

Torkzaban, S., Hassanizadeh, S., Schijven, J., van den Berg, H., 2006. Role of air–water interfaces on the retention of viruses under unsaturated conditions. Water Resources Research 42, 1–11.

Torkzaban, S., Kim, H., Simunek, J., Bradford, S., 2010. Hysteresis of colloid retention and release in saturated porous media during transients in solution chemistry. Environmental Science and Technology 44, 1662–1669.

U.S. Army Corps of Engineers, 2008. HEC-RAS — River Analysis System. Technical Report.Davis, CA.

USEPA, 2004. Comprehensive surface water treatment rules (SWTR) quick reference guide: systems using slow sand, diatomaceous earth, or alternative filtration. Technical Report. United States Environmental Protection Agency (USEPA), Washington, D.C., USA.

van Genuchten, M., 1980. A closed-form equation for predicting the hydraulic conductivity of unsaturated soils. Soil Science Society of America Journal 44, 892–898.

via donau, 1997. Die kennzeichnenden Wasserstände der österreichischen Donau (KWD 1996). Technical Report. (Vienna, Austria).

Voss, C.I., Provost, A.M., 2008. SUTRA – a model for saturated – unsaturated variable-density ground water flow with solute or energy transport. Technical Report Water-Resources Investigations Report 02-4231. (Reston, Virginia).

Weiss, W., Bouwer, E., Aboytes, R., LeChevallier, M., O'Melia, C., Le, B., Schwab, K., 2005. Riverbank filtration for control of microorganisms: results from field monitoring. Water Research 39, 1990–2001.

Woessner, W., Ball, P., DeBorde, D., Troy, T., 2001. Viral transport in a sand and gravel aquifer under field pumping conditions. Ground Water 39, 886–894.

Yao, K., Habibian, M., O'Melia, C., 1971. Water and waste water filtration: concepts and applications. Environmental Science and Technology 5, 1105–1112.